

NIRCAM-IFTS: Imaging Fourier Transform Spectrometer for NGST

Winfried Posselt

Dornier Satellitensysteme, Ottobrunn, Germany

Jean-Pierre Maillard

Institut d'Astrophysique, Paris, France

Gillian Wright

Astronomy Technology Centre, Edinburgh, UK

Abstract.

NASA has invited ESA to extend their successful collaboration on HST to the NGST project, and ESA has undertaken a number of assessment studies which aimed at defining its potential instrument and spacecraft hardware contributions to the NGST mission. One of these ESA studies called "Study of Payload Suite and Telescope for NGST" (ESTEC/Contract No. 13111/98/NL/MS), has been conducted by Dornier Satellitensysteme (DSS), together with Alcatel Space (AS), and a team of 16 European science institutes chaired by Laboratoire d'Astronomie Spatiale (LAS) and UK Astronomy Technology Centre (UK-ATC). DSS took the responsibility for the overall study and the payload, AS for the telescope, and the science team was responsible for the instrument and telescope definition and requirements.

The NIRCAM-IFTS is one out of four instruments that were defined by the science team as potential NGST payload and were detailed by DSS. This document discusses the optical and opto-mechanical design and analyses of the instrument. Technical aspects that are common to instruments studied by DSS are described in separate reports ("NGST Payload Study, Final Report" and Posselt et al. 2000).

1. Introduction

The NASA Design Reference Mission has been defined to help set the science requirements defining the instrument payload. A large fraction is a core program, designed to understand the origin and evolution of galaxies, mapping dark matter, measuring cosmological parameters and study the physics of star formation. The DRM also includes a range of other studies which fall within the NASA Origins program. Since it is difficult to anticipate in detail the most important studies at the time of launch, some flexibility in the instruments is required. An IFTS can provide some of this in the form of variable spectral resolution, and in

its ability to carry out spectroscopic surveys unbiased by selection effects. We list some of the DRM programs for which an imaging FTS would be suitable.

- NGST will be uniquely capable of both discovering and obtaining spectroscopy for distant supernovae (SN) with $z \sim 2-4$, a region which will yield more definitive cosmology tests than those reachable by ground based surveys. Deep wide field images will play a key role in finding distant SN, but identifying the SN and their type will also require low resolution wide band-width spectroscopy. SN searches will thus require wide field surveys with both photometric and spectroscopic information, tasks which could potentially be carried out simultaneously with an imaging FTS.
- Deep imaging and spectroscopic surveys in the near-IR are needed to study galaxy formation and evolution for field and cluster galaxies, the effects of AGN on chemical evolution and to understand the nature of gamma-ray burst sources. This is an area where the deep imaging capabilities of NGST, coupled with spectroscopic information are likely to open new areas of study, based on “serendipitous” discoveries found in the deep images.
- NGST will provide the first opportunity to study the detailed properties of proto-planetary disks as a function of age, stellar mass and environment. These studies require both good photometric imaging and low resolution spectroscopy across the full 1–5 μm band, as well as in the mid-IR, and so an imaging FTS would be suitable for this.

2. Imaging FTS Technical Specifications

The concept of an FTS was felt to be particularly attractive if it were able to combine sensitive imaging in broad bands with low resolution spectroscopy up to $R \sim 300$. If the number of instruments in the NGST payload suite is limited, then combining two functions in a single instrument might be an efficient use of resources. Since broad band near-IR imaging capability is at the core of so much NGST science it is important not to compromise performance if an IFTS is to be used as the camera. Thus this IFTS was required to provide the same performance for broad band imaging, with the same number of detectors, as the near-IR camera which was also part of this study. All the detectors are placed at a single output port and imaging with the same throughput as a simple camera is then achieved by setting the FTS to zero path difference (constructive interference ensures that all of the light reaches the detector) and using a broad band filter. As with the camera, it was considered important to keep the instrument simple with a fixed spatial sampling. For narrow band imaging the images are reconstructed from very low resolution spectra taken by scanning the FTS. This is less efficient than using a narrow band filter, but on the other hand it allows any central wavelength and bandpass to be selected. Again with simplicity in mind, provision for only low resolution spectroscopy (R up to ~ 300) was considered. Based on these considerations the high level specifications for the IFTS are as given in Table 1.

Table 1. NIR FTS High Level Specifications

Item	Specification
Wavelength Range	0.6–5 μm
Field of View	3×6 arcmin
Spatial sampling	0.03 arcsec/pix
Filters	Broad band (...JHK...)
Resolution	5 to 300
Sensitivity	in broad band imaging mode: same as filter wheel camera

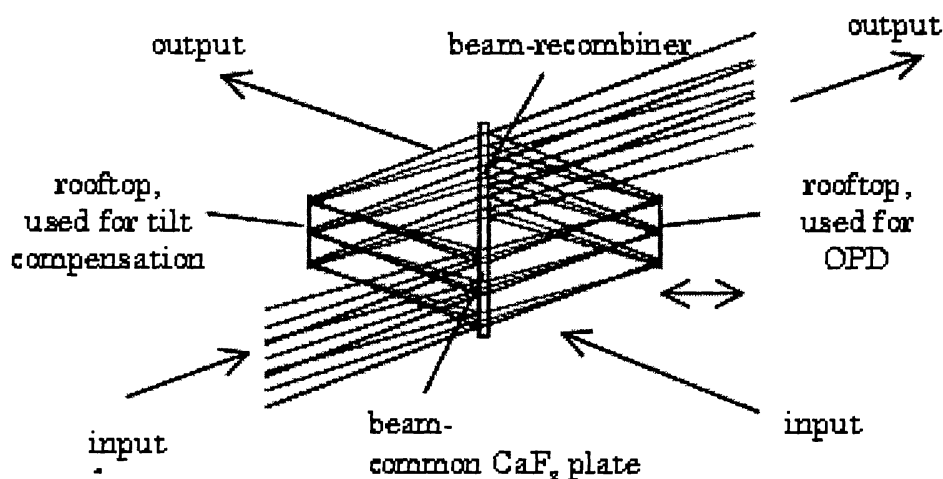


Figure 1. Interferometer optical design; at ZPD position there is constructive interference of all spectral elements in output port 1.

3. Interferometer Optical Design and Analyses

The interferometer is a Mach-Zehnder configuration with two input and two output ports, although the actual instrument design is restricted to a single output port. Its principle design is shown in Figure 1.

The interferometer optics consist of a CaF₂-plate with identical coatings for beam-splitting and beam-recombining, a fixed and a moving retro-reflector. The input radiation is amplitude divided by the beamsplitter. A variable, time dependent Optical Path Difference (OPD) is introduced between the two parts of the divided input beam by mechanical movement of one retro-reflector. Then, both parts of the input beam are recombined at the beam-recombiner and brought to interference: the time dependent OPD variations result in time

dependent intensity fluctuations at the focal plane. Inverse Fourier transformation of the interferometric signal retrieves the original spectrum with a spectral resolution depending on the maximum OPD between the two beams.

Rooftops are preferred as retro-reflectors rather than plane mirrors, since they are insensitive to small tilt angles around the rooftop intersection line and require tilt control only around the axis perpendicular to the paper. One of the rooftops will be used to adjust the tilt angle around this axis.

3.1. Camera Mode

In camera mode the OPD is kept at zero (ZPD position of rooftops). This will result in constructive interference of all input radiation in the symmetrical output port 1. In this mode the interferometer is optically not present and the efficiency is comparable to a broad band filter wheel camera. The first task when operating the IFTS is thus to determine the ZPD position and to minimize the effect of tilt. In practice this can be an automated sequence searching for the ZPD peak of the interferogram when all filters are removed (this will provide a very distinct peak, see the figure on the right showing the FFT of a broad band Planck function) and then find the tilt position for maximum ZPD amplitude.

3.2. Interferometer Mode

The retro-reflector is moved from ZPD position in one direction only, thus creating “single sided” interferograms. Besides a somewhat lower readout noise contribution this concept has an operational advantage: the IFTS will start to gather broad band image information at ZPD, and the spectral details will increase with increasing OPD (i.e., with time). The measurement of an interferogram can be stopped at any OPD position, and can later be continued if further spectral information is required (in this case a few samples at ZPD will be needed for calibration purposes). The imaging performance of the optical system is not affected in the interferometer mode, i.e., the full spatial information of the camera mode will also be available in this mode.

In interferometer mode the second output port contains the same information as the first port and can be used independently from the first port. In the actual design these enhancement capabilities have not been further detailed, and the second input and output ports are both blocked by plates of high emissivity, thus simulating quasi-zero radiation sources.

3.3. Interferometer Design Requirements

The interferometer opto-mechanical design is shown in Figure 2; indicated are the relevant mechanical design requirements. Although the Mach-Zehnder configuration introduces shear during OPD acquisition, the optical design tolerates a mechanical stroke of several mm without significant performance degradation.

Optical references for OPD measurement are critical elements at NGST conditions. On the other hand, the expected in-orbit thermo-mechanical conditions are much more stable than in any laboratory on ground. An interesting alternative to an optical reference is thus to rely on the mechanical stability of the interferometer and measure the OPD with a mechanical device like the capacitive nanosensors of Queensgate. A high thermo-mechanical stability of

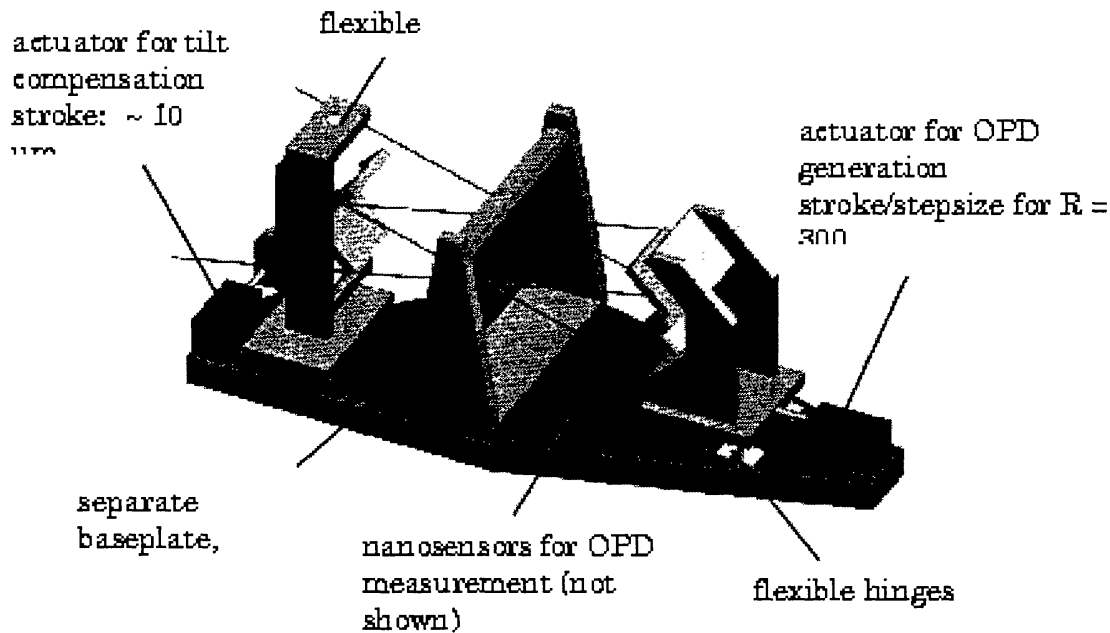


Figure 2. Interferometer opto-mechanical design.

the interferometer unit can be achieved by isostatic mounting of the unit, providing thermal and mechanical decoupling from the instrument baseplate. First estimates demonstrate the feasibility of this option.

3.4. Optical Instrument Design

The optical configuration of the NIRCAM-IFTS is based on the scientific performance requirements of Table 1 and shown in Figure 3. It is a common design for both the camera and the FTS operation mode. The functional units of the instrument optics are the collimator, the filter wheel, the interferometer and the imager. The collimating and imaging optics are slightly different tele-objective designs with focal lengths of 1.7 m. They consist of two aspherical mirrors which are not critical for manufacturing. The entrance and exit pupils are telecentric. The aperture stop of the system is at the intersection line of the rooftops, keeping the interferometer as compact as possible. The collimating optics have been optimized to produce a beam of good parallelism at the interferometer. The filter wheel is located in the parallel beam between the collimating optics and the interferometer optics. It contains 8 standard astronomical broad band filters and one empty position for alignment purpose and to determine the ZPD position for the camera mode.

Two folding mirrors arranged under an angle of 45° are used to get the focal plane close to the optics on a common baseplate. These two mirrors are mechanically connected and movable by means of a refocusing mechanism to focus the beam on the detector array, if necessary after cool down.

The optical performance of the image is diffraction limited. The Strehl ratios exceed 0.83 across the whole field. The MTF as a function of frequency calculated at the center and corners of the field is given in Figure 4. At all field positions the MTF is fairly close to the diffraction limit.

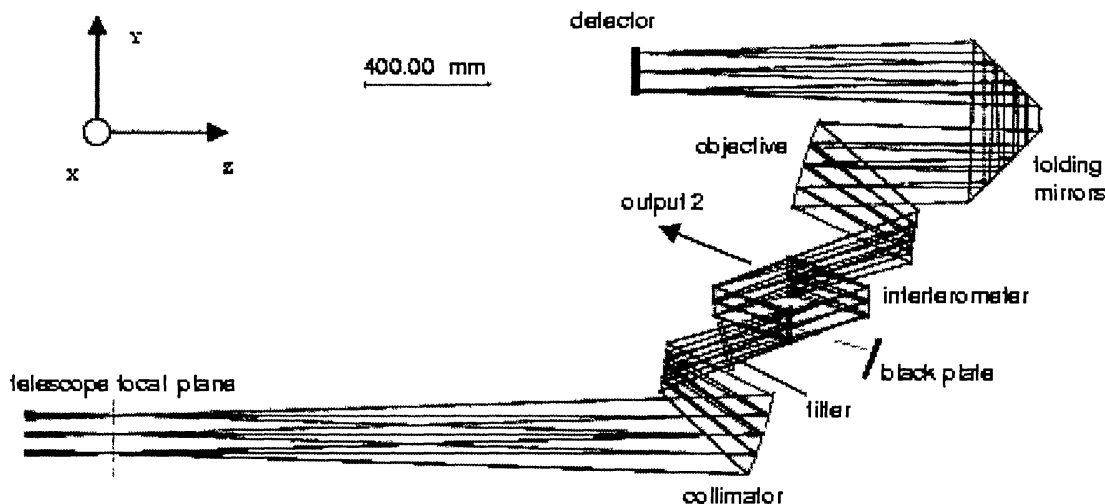


Figure 3. NIRCAM-FTS optical configuration; field size: $6' \times 3'$ in X/Y dir.

Table 2. Summary of IFTS Design Parameters

Parameter	Value
wavelength range	1 to 5 μm
reduction ratio	1
f-number at object side	16
field (arcmin)	$6' \times 3'$
detector arrays	12K \times 6K
pixel size	18.5 μm
IFOV	0.14 μrad (or 30 mas)
entrance/exit pupil	telecentric
stop	at rooftops
stop diameter	100 mm
beam-splitter & beam-recombiner	common CaF_2 plate, ident. coating designs
spectral filters	filter wheel with 8 broad band filters and one blank position

The modulation efficiency (ME) is a measure of the contrast of the interference fringes. A value < 1 is caused by phase differences across the wavefronts of the two interfering beams, and has an effect on the instrument sensitivity. A reduction of the ME is caused by wavefront shear and tilt, wavefront error and beamsplitter performance. Table 3 below lists the proposed performance requirements. Most critical is the wavefront error at short wavelengths because of its exponential characteristic. Including the ME, the mean overall transmission at 1 μm is ~ 0.75 in camera mode, and ~ 0.38 in interferometer mode (single port design).

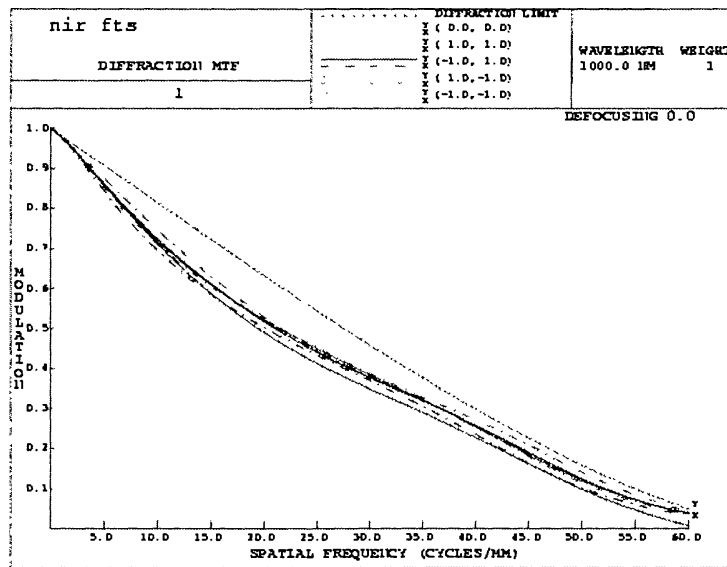


Figure 4. MTF as a function of spatial frequency.

Table 3. Proposed Performance Requirements to get ME > 92% at 0.6 μm

	Requ. Performance	modulation Efficiency	Comment
shear	< 1 mm	> 0.99	uncritical
tilt	< 0.5 μrad	> 0.99	in-orbit adjustment capability required
wavefront error	< 30 nm rms	> 0.95	good beamsplitter planarity required
beamsplitter	0.45 < R, T < 0.55	> 0.99	uncritical

4. Photometric Performance

The expected in-orbit instrument performance is shown in Figure 5. The model includes all instrument and telescope efficiencies. The expected zodiacal light background¹

has also been considered. The performance of both the camera and interferometer mode is for all target magnitudes photon noise limited. In interferometer mode the whole target and background radiation within the selected broad band will reach the detector—there is no difference to the camera mode. In the faint

¹From the NGST Exposure Time Calculator

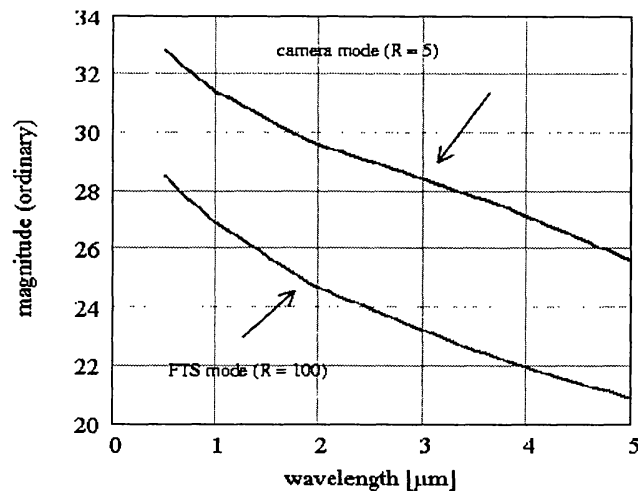


Figure 5. Magnitudes (ordinary!) of point sources vs. wavelength resolved in camera and IFTS mode with $\text{SNR} = 10$ and 10^5 sec observation time. In FTS mode all 20 low spectral resolution elements within a broad band are recorded simultaneously.

object limit of Figure 8 the zodiacal light is the dominating noise source. The detector and the readout noise are negligible.

5. Opto-Mechanical Design

The baseline opto-mechanical designs are shown in Figures 6 and 7.

The optical bench as primary structure consists of a light-weighted plate made of C/SiC material. The mirrors are connected to C/SiC brackets by an isostatic 3 point support. Flexible INVAR mounts are used as connection elements. The two folding mirrors are mounted on a separate C/SiC plate which can be moved by a mechanism for optics refocusing.

6. Instrument Budgets

7. Conclusions

The presented Imaging Fourier Transform Spectrometer has very good imaging quality. The interferometer optics is a rather compact Mach-Zehnder configuration which works well as a Fourier Transform

Spectrometer—given the small stroke of the moving mirror and the good quality of the interfering optical beams. This rather compact interferometer optics consists of planar surfaces only and can be built and tested as a separate module.

The main IFTS design and performance features are:

- + high image quality in camera and spectrometer mode

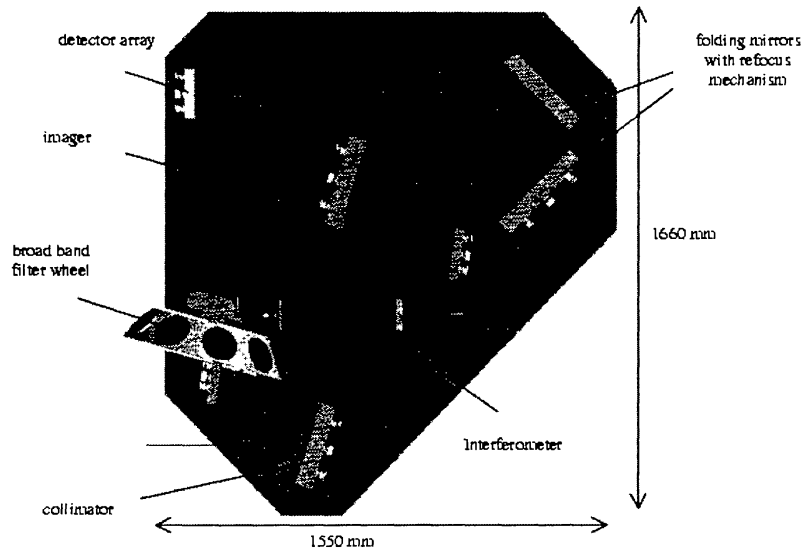


Figure 6. NIRCAM-FTS design: top view.

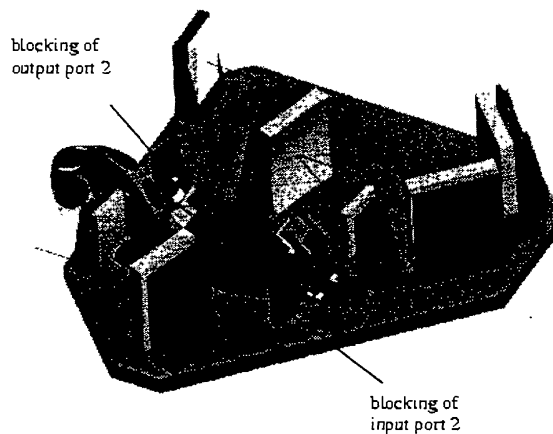


Figure 7. NIRCAM-FTS design: 3D view.

- + high spectral quality and easy spectral calibration (achromatic interferometer optics, all spectral information on the same detector pixel)
- + low sensitivity against detector noise, internal straylight and particle impact (after FFT the signal offset is distributed across all spectral elements)
- + compact interferometer of high stability tolerates simple OPD measurement system (mechanical measurement)

Table 4. Estimated Instrument Budgets

Parameter	Estimated budget figure
Dimensions	$1.66 \times 1.55 \times 0.58 \text{ m}^3$
Mass	88 kg (assuming C/SiC material)
Average Power (analog part only)	FPA: 25 mW, ASP & control: 18.2 W
Heat Load on Radiator	31 mW at 30 K
Science Data Rate	1.8 Gbit/1000 sec
Downlink memory	72 Gbit (80 frames/day, compressed)

+ enhancement capabilities, making use of the second output port

- low efficiency in case not all spectral information within a selected broad band is needed (this would require additional narrow band filtering)

Acknowledgments. The work has been performed under ESA contract for the “Study of Payload Suite and Telescope for NGST.” ESA study manager was J. Cornelisse, ESA study scientist was P. Jakobsen. We would like to particularly thank D. Elbaz, P. van der Werf, J. L. Puget and L. Vigroux for their contributions as part of the science team to the concepts presented here.

References

- “Study of Payload Suite and Telescope for NGST,” ESTEC/Contract No. 13111/98/NL/MS
- “NGST Payload Study, Final Report,” NGST-FR-DSS-PST-001, Issue 1, 22-Oct-99
- Posselt, W., et al. 2000, these proceedings